ISBN: 978-3-95450-168-7 doi:10.18429/JACoW-IPAC2015-TUPMA055

ANALYSIS OF POSSIBLE BEAM LOSSES IN THE NSLS II STORAGE RING

Y. Li, S. Seletskiy#, W. Guo, R. Fliller, S. Kramer, B. Podobedov, T. Shaftan, B. Wahl, F. Willeke,
BNL, Upton, NY 11973, USA

Abstract

The NSLS-II accelerators are installed within radiation shielding walls that are designed to attenuate the radiation generated from an assumed beam loss power to a level of <0.5mrem/h at the outer surface of the bulk shield walls. Any operational losses greater than specified level are expected to be addressed by installing supplemental shielding near the loss point in order to attenuate the radiation outside the shield wall to the design level. In this paper we report the analysis of the electron beam missteering in the NSLS-II Storage Ring for the determination of supplementary shielding.

INTRODUCTION

The missteering (caused by operator's mistake or by a magnet failure) of the electron beam freshly injected into NSLS-II Storage Ring (SR) [1] can result in unacceptable radiation levels on experimental floor. Design of respective radiation protection shielding [2] relies on detailed analysis of physically possible steering errors. In this paper the potential angles and offsets of the missteered beam are calculated by implementing the cascaded parameter scan (CPS) [3]. This method was originally developed for the top-off safety analysis, was realized in a parallel python code and benchmarked with other top-off safety simulators developed in SLAC and LBNL. The results of the studies were double-checked with independent simulations using simplified magnets fields profiles and a smaller number of tracked beam particles (explained below). The detailed description of the analysis results is given in [4].

SR DESCRIPTION

Figure 1 schematically shows the lattice of NSLS-II Storage Ring. The SR lattice contains 30 double bend achromats (DBA). There are 15 short straight (low-β) and 15 long straight (high-β) sections.

The storage ring is designed to accept 3GeV electron bunches from the Booster. An interlock in the Booster to Storage Ring transport line [7] constrains the injected beam energy within a window of 2 - 3.15GeV.

Our analysis is based on particle tracking, which is performed by solving a set of ordinary differential equations describing electron motion in magnetic field. The magnets field profiles are obtained from their 3D models. To simplify the calculation while keeping the adequate accuracy [5, 6] we use 1D transverse profiles for quadrupoles and sextupoles and 2D profile for dipoles in the horizontal middle plane. Figure 2 shows magnetic fields used in the simulations.

The dipole power supply current and voltage are interlocked within 2% window. Each dipole has a back-leg winding, which can contribute ≤ 3% field variation. The total possible dipole field range scanned was chosen as ±5% around its nominal setting.

The range for the other SR magnets was set by the maximum current of their power supplies and their possible magnetic fields, as listed in [4].

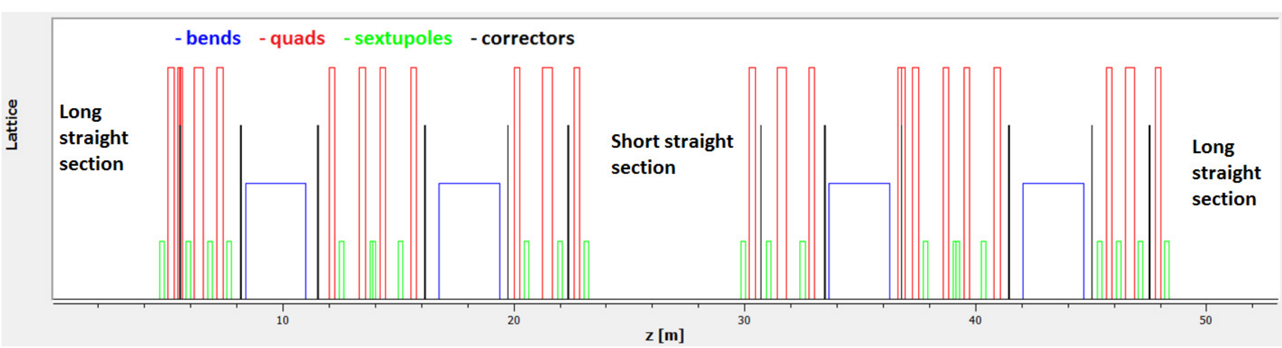

Figure 1: NSLS-II SR lattice.

BEAM STEERING ANALYSIS

The CPS utilizes the following beam tracking algorithm. We start with the phase space of beam trajectories defined by the geometric acceptance of the long straight section. Such phase space area covers all possible incident beam trajectories.

Next, we track trajectories within the phase space through the first beamline element varying its field and the beam energy over their full range. We record each beam trajectory's coordinates in phase space after it passes the magnet and find the maximum angle and position of trajectories not intercepted by the magnet yoke. Then we discard the trajectories that were lost on the vacuum chamber and the surviving trajectories define a phase space volume. This phase space was used to

#seletskiy@bnl.gov

ISBN: 978-3-95450-168-7 doi:10.18429/JACoW-IPAC2015-TUPMA055

generate new particles within volume for tracking through the next downstream magnet. We repeat the same procedure until the end of the beam-line is reached.

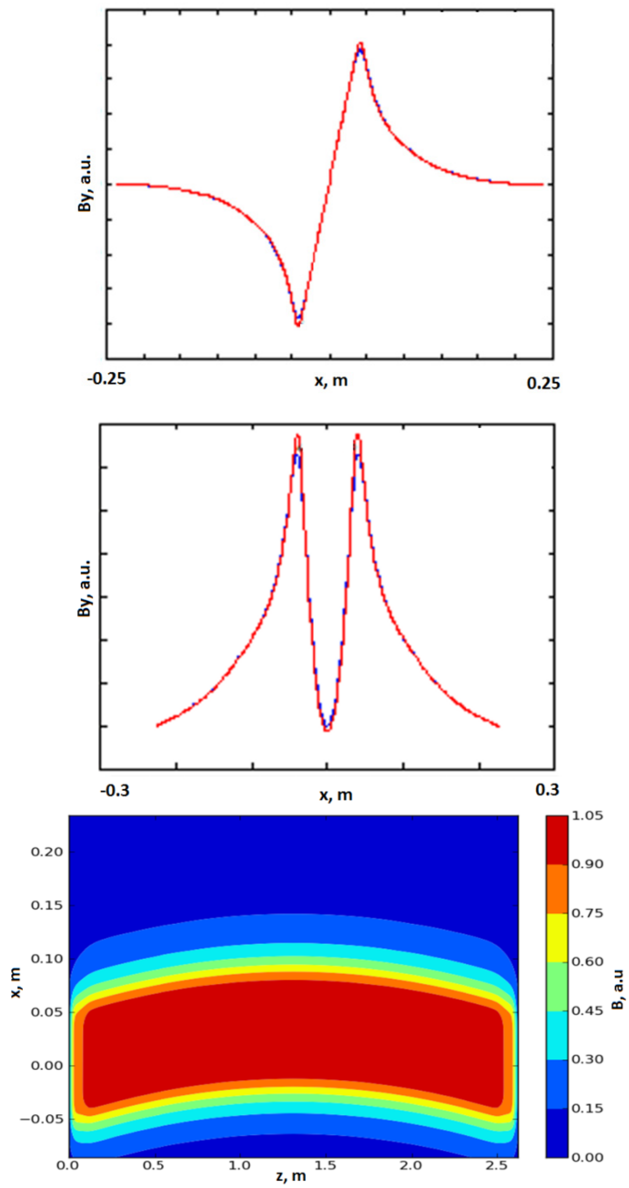

Figure 2: Profiles of magnetic field for quadrupole (top), sextupole (middle) and dipole (bottom) in the SR.

For the physical apertures confining the beam along a beam-line we used the vacuum chamber or synchrotron radiation absorbers in drift spaces between two adjacent magnets or the magnet yokes inside the magnets. The vacuum chamber had a large asymmetry with a vacuum pumping and photon beam extraction slot to the outside of the ring.

At the downstream end of each beamline element, the phase space was repopulated to exclude exponential growth of the number of beam trajectories and to ensure that the number of trajectories stays approximately the same throughout the whole tracking routine.

The method of repopulating the phase space, a so-called “phase space sand moulding”, is schematically shown in Fig. 3. The main idea of this method is to create a phase space area, which has an identical shape to the area of initial phase space but contains a smaller number of equally spaced beam particles.

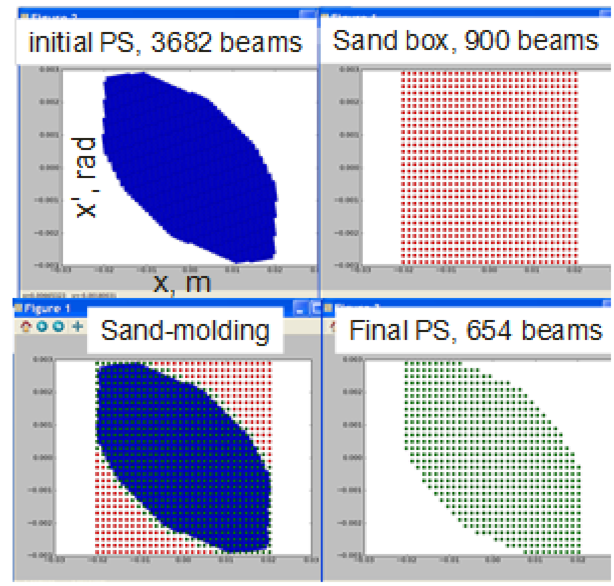

Figure 3: In sand-moulding technique the repopulated phase space is obtained by “imprinting” the original phase space on the “sand box” of beam particles.

We performed the tracking studies separately in the horizontal and vertical planes. Figure 4 illustrates the tracking.

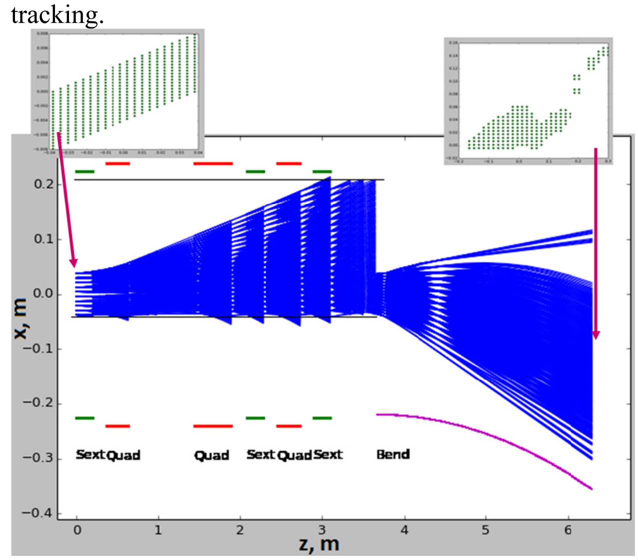

Figure 4: CPS horizontal tracking through the beginning of the long straight and first dipole. Green, red and magenta lines show respective yokes of quads, sextupoles and the dipole. Most beam losses happen in the drifts on the vacuum chamber (grey lines) or photon apertures. The two upper plots show beam trajectories phase spaces at the beginning and at the end of the beamline. For illustration purposes the tracking was performed with only 200 trajectories.

ISBN: 978-3-95450-168-7 doi:10.18429/JACoW-IPAC2015-TUPMA055

For each plane, we carried out tracking for one period (consisting of two cells) starting from the long straight section. The reason of using only one super cell is that the missteered beam has the same loss pattern for all 15 identical periods. This analysis covers possible losses in the SR injection section as well, since the phase space area defined by the geometric acceptance of the long straight section is larger than the maximum possible phase space area of beam exiting the pulsed injection septum. The studies of the SR DC and pulsed injection septa missteering are covered in [8].

For the horizontal direction we carried out a tracking study in the middle plane because the maximum apertures always occur at this plane. The possible displacement in the vertical plane has been taken into account by increasing the magnet scanning ranges [3, 5 and 6]. For tracking in vertical direction we substituted dipoles with the drifts and changed quads and sextupoles polarities to the opposite ones. Since the parameter scan is done for dual polarities for all multipoles it is unnecessary to distinguish focusing and de-focusing magnets. It is worth to point out that in the vertical plane the tight sextupole and dipole yokes apertures constrain e-beam motion within much smaller angles as compared to the horizontal plane.

Our analysis showed that the largest possible beam deflections are found at exits of the bends. The horizontal beam angles in these locations can be as high as 120 mrad. Figure 5 shows our simulations results for surviving particle (for all energies and range of magnet settings) at the exit of the first dipole.

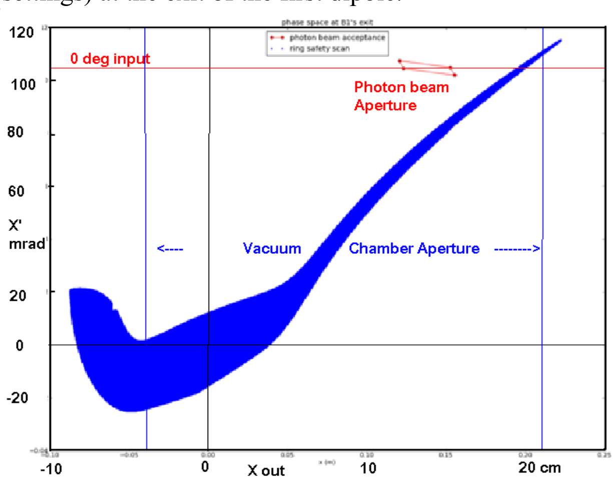

Figure 5: Beam particle phase space (blue dots) at the exit of the first dipole. Also shown are the photon beam aperture around the input beam direction and the dipole vacuum chamber apertures.

The obtained maximum beam deflections for each SR magnet were used for the analysis of possible radiation losses and for the design of respective radiation protection shielding [2]. In most cases, subsequent magnet yokes provided an adequate beam absorber to minimize the radiation toward the outside of the ring. However, the beam line extraction ports (exit of the dipoles) provided little material to absorb the potential high energy beam losses toward the outside of the SR. This necessitated installation of lead dipole shadow shields (DSS) to absorb and soften the intense radiation cone in the forward beam direction.

Figure 5 showed that under possible operating range of the magnetic elements and the potential range of beam energies, miss-steered injection beam cannot pass down the photon beam line (aperture shown in Fig. 5). However, the extreme particle trajectories will be intercepted by the DSS, avoiding extremely high levels of radiation in the user first optical beam enclosures, even with the photon and bremsstrahlung shutters closed (i.e. occupancy of the enclosure permitted)[2].

A complimentary study was carried out to search for the possible electron beam losses. In that study each magnetic element in the ring was treated as a dipole magnet. The deflection angle was calculated from the maximum possible kick of the magnet. The kick was swept from negative to positive polarity, and the phase space envelope was respectively enlarged at the end of the element. In this study the tracking was not stopped if particle hit aperture; instead the penetration depth in the material was recorded. The study confirmed locations where lost beam was not effectively shielded.

CONCLUSIONS

In this paper we presented the studies of possible beam missteering and beam losses in NSLS-II Storage Ring. We applied the cascaded parameter scan approach to determine beam's maximum steering angles and offset at each SR magnet. The found possible beam displacements were used for analysis of potential radiation losses in the SR and for design of the respective radiation shielding. Commissioning and operation of NSLS-II gave an ultimate proof of the adequacy of the resulting radiation shielding.

ACKNOWLEDGEMENTS

We are grateful for support from NSLS-II. We obtained a lot of support and advice from M. Breitfeller. This work is supported in part by the U.S. Department of Energy (DOE) under contract No. DE-AC02-98CH1-886.

REFERENCES

[1] NSLS-II CDR, 2006.
[2] S. Kramer, et al,, "Shielding Specification and Design Document for the BSR-P2 and Storage Ring" LT-C-ASD-RSI-SR-001, 2013.
[3] Y. Li, L. Yang, and S. Krinsky, Phys. Rev. ST Accel. Beams 14, 033501 (2011)
[4] Y. Li, S. Seletskiy, "Analysis of Mis-Steered Electron Beam in the NSLS-II Storage Ring" NSLS-II Tech. Note. 122, 2013.
[5] H. Nishimura et al., Nucl. Instrum. Methods Phys. Res., Sect. A 608, 2 (2009)
[6] Y. Li et al., NSLS-II Top-off Safety Study Report.
[7] S. Seletskiy et al., WEPRO020, IPAC14, 2014.
[8] S. Seletskiy et al., TUPMA056, IPAC15, 2015.